Proceedings of the IISE Annual Conference & Expo 2022
K. Ellis, W. Ferrell, J. Knapp, eds.

Predictive Modeling of Additive Manufacturing Process using Deep Learning Algorithm

Michael Ogunsanya[a] and Salil Desai[a]

[a] *North Carolina A&T State University, Greensboro, North Carolina, USA*

Abstract

Fused deposition modeling (FDM) is one of the widely used additive manufacturing (AM) processes but shares major shortcomings typical due to its layer-by-layer fabrication. These challenges (poor surface finishes, presence of pores, inconsistent mechanical properties, etc.) have been attributed to FDM input process parameters, machine parameters, and material properties. Deep learning, a type of machine learning algorithm has proven to help reveal complex and nonlinear input-output relationships without the need for the underlying physics. This research explores the power of multilayer perceptron deep learning algorithm to create a prediction model for critical input process parameters (layer thickness, extrusion temperature, build temperature, build orientation, and print speed) to predict three functional output parameters (dimension accuracy, porosity, and tensile strength) of FDM printed part. A fractional factorial design of experiment was performed and replicated three times per run (n=3). The number of neurons for the hidden layers, learning rate, and epoch were varied. The computational run time, loss function, and root mean square error (RMSE) were used to select the best prediction model for each FDM output parameter. The findings of this work are being extended to online monitoring and real-time control of the AM process enabling an AM digital twin.

Keywords

Additive manufacturing, fused deposition modeling, deep learning, multi-layer perceptron, hyperparameter tuning.

1. Introduction

Additive manufacturing is a bottom-up layer-by-layer manufacturing method [1] [2]. Fused deposition modeling (FDM) is classified as a type of material extrusion additive manufacturing according to the American Society for Testing and Materials (ASTM) [3]. FDM involves the heating of plastic material referred to as filament to its glass transition temperature where it could be forced out through the nozzle of the extruder. Printing is done according to the tessellated programmed profile after slicing the previously prepared computer-aided design (CAD). Fused deposition modeling is one of the most widely used additive manufacturing process based on its ease of use and its relative lower acquisition cost [4]. Both functional and non-functional parts have been printed with FDM although there are limitations to its applications [2].

With industrial internet of things (IIoT) sensors, it is easier to capture data in different formats [5], [6]. Also, with the availability of high-performance computational servers and state-of-the-art machine learning algorithms, understanding of complex and dynamic processes such as the additive manufacturing have been a well-researched [7]. Machine learning has been used in different fields to understand the complexity and nonlinearity that exist in a system when sufficient data are provided [8], [9]. It serves as a black box for decoding the relationship between input parameters and outputs parameters without the need for understanding of the science around the phenomenon in the system domain. Machine learning has been applied in additive manufacturing to study how the output parameters are influenced by the input parameters combination sets [10].

Deep learning is a type of machine learning that is patterned around the biological neurons of the human brain. Deep learning has also easily be applied in different areas of additive manufacturing processes [11]. The multilayer perceptron architecture is one of the deep learning algorithms, consisting of an input layer, one or more hidden layers, and an output layer. The number of neurons for the input layer corresponds to the number of considered input parameters. The number of hidden layers and number of neurons for each hidden layer depend on the complexity of the relationship between the input parameters and the output. In most cases, number of hidden layers are chosen based on experience or rule of thumb. The number of neurons for the output layer depends on the number of output parameters. Hyper-parameter tuning is an act of having an appropriate setting for the model parameters for efficient

and effective use of computation resources and obtaining the desired output. The fused deposition method can be affected by the slightest change in input process parameters. Thus, it is vital to predict the output parameters based on variations in the input parameters within the shortest time, computational resource usage, and the need for additive manufacturing hyperparameter tuning.

2. Background Research

Most works found in the literature concentrate on predictive modeling in additive manufacturing process without investigating the hyperparameter tuning which is key if the model is to be incorporated in real-time for a digital twin. [12] used data-driven approach to predict surface roughness in fused deposition modeling using random forest. [13] used an ensemble learning algorithm to predict surface roughness using multiple sensors such as thermocouples, infrared temperature sensors, and accelerometer to measure both temperature and vibration data. Surface prediction was predicted in an additive manufacturing process using wired arc additive manufacturing [14]. [15] optimized both surface roughness and dimension accuracy in a Laser powder bed fusion (LPBF) using whale swarm optimization. Three algorithms, adaptive neuro-fuzzy inference system (ANFIS), extreme learning machine (ELM), and support vector regression (SVR) were used to predict the surface roughness [16]. Also, genetic algorithm (GA) and particle swarm optimization (PSO) were used to optimize the predictive function. Gaussian process-based prediction was used for porosity prediction in an additive metallic manufacturing process using selective laser melting (SLM) [17]. Both convolutional Neural Network (CNN) and Residual-Recurrent Convolutional Neural Networks (Res-RCNN) using transfer learning were used on thermal images for porosity prediction in real-time [18]. [11] used long short-term-based predictive model to predict tensile strength of printed parts using fused deposition modeling. The LSTM model outperformed both support vector regression and random forest. [19] used temperature history of the weld interface was used to predict the strength of printed parts using FDM. Different optimization techniques have been applied to hyperparameter tuning but two widely used techniques are random search [20] and Bayesian Optimization [21]. This research is focused on tuning with all hyperparameter combination.

3. Methodology

In this research, critical input parameters for fused deposition modeling were selected based on a detailed literature review. The selected input parameters included (a) layer thickness, (b) build orientation, (c) build temperature, (d) extrusion temperature, and (e) print speed. Three prominent output parameters were chosen which include (a) dimensional accuracy, (b) porosity, and (c) tensile strength. For each factor, three levels were chosen to represent low, medium, and high. A fractional factorial design was conducted with 3^{5-1} = 81 runs. Each run was replicated three times (n=3) with 243 total data points. Candidate data fields from the total dataset are shown in **Table 1**. Also, **Figure 1(a)** shows the multilayer perceptron architecture used in this work and its exploration by varying the number of hidden layers, number of neurons in each hidden layer, other hyperparameters (e.g., learning rate and epoch). For each variation, both the root-mean square error (RMSE) value and computation run time were computed and used as output metrics to choose the best hyperparameter combination for each of the output parameters.

Table 1: First five combinations run considering five (5) input parameters and three (3)

	Input/process parameters					**Mean Output**		
	Layer thickness (mm)	**Build orientation** ($degree$)	**Build temperature** (℃)	**Extrusion temperature** (℃)	**Print speed** (mm/s)	**Dimensional accuracy** (%)	**Porosity** (%)	**Tensile Strength** (MPa)
1	0.2	0	30	160	25	7	13	29
2	0.2	0	30	180	50	4.5	9.5	33.5
3	0.2	0	30	200	75	6.5	11	30.5
4	0.2	0	60	160	50	7.5	13	29.5
5	0.2	0	60	180	75	4	8.5	32.5

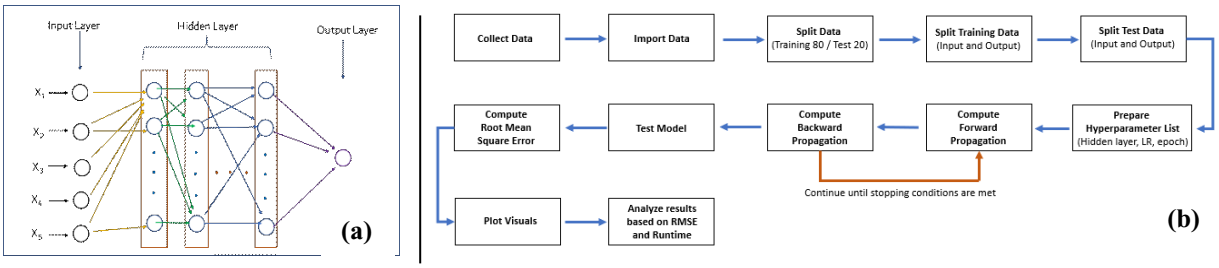

Figure 1: (a) Multilayer perceptron architecture with five input neurons at the input layers, varying number of hidden layers and number of neurons in each hidden layer, and one neuron for the output layer **(b)** Steps used on the fused deposition additive manufacturing data set **(b)** shows the steps to model the relationship between the critical input parameters and the output parameters. The input data were standardized between 0 and 1 to facilitate the multilayer perceptron learn faster which in turn aided faster convergence of the loss function for the given number of epochs.

4. Results

The learning status of each algorithm was evaluated based on changes to the hyperparameter. The predictive model is only considered if the status is "L", that is, "Learning" as shown in **Table 2, 3 and 4**. Learning is defined when the model can learn through the training dataset at the set conditions of number of neurons for each hidden layer, learning rate, and epoch. If the status is "NL", that is, "Not learning", the predictive model is discarded.

For a single hidden layer, as illustrated in **Table 2**, the learning rate plays a crucial role in the prediction for the output factor "dimensional accuracy." Increasing the number of neurons from 3 to 5 or 8 or increasing the number of epochs beyond 5000 does not improve the RMSE although the runtime stands at 1.9 s for those combinations. From the learning status, the multilayer perceptron does not learn at a learning rate of 0.001 and below irrespective of other hyperparameters. For porosity and strength predictions, learning rate is key as their best RMSE values were at 0.0001 while, LR = 0.00001 increased the runtime beyond 3.19 s and 5.37 s, respectively, at other chosen hyperparameters.

For the model with two hidden layers (**Table 3**), considering dimension accuracy, a good combination of hyperparameters setting were obtained at learning rate of 0.0001, number of epochs at 5000, second hidden layer at 3. The first hidden layer with 3 neurons had RMSE value of 1.89 with a runtime of 2.19 s but with 5 neurons, a better RMSE value (1.44) was obtained at an increased runtime to 2.36 s. With increased number of neurons to 8 in each hidden layer, no learning was recorded. Porosity prediction tends to improve with an increase in the number of neurons in the first hidden layer having second hidden layer with 3 neurons, learning rate at 0.0001, and number of epochs at 5000. RMSE values as 3.59, 2.21, and 1.94 with runtime of 2.16, 2.41, and 2.40 s, respectively. For the strength prediction, learning rate is key as there was no learning at other learning rates except at 0.00001. The best RMSE value was obtained as 6.4 at most hyperparameter combinations.

For three hidden layers (**Table 4**), although there were much RMSE improvements but resulted in extreme high runtime. For instance, for dimension accuracy prediction, a RMSE of value of 1.26 was obtained at a learning rate of 0.00001 and at 25000 epochs with all hidden layers having 3 neurons. This took about 42 seconds. All superior results occurred with both learning rate of 0.00001 and 25000 epoch. Though, an improved RMSE value of 1.73 was obtained compared to one and two hidden layers was obtained with all hidden layer having 3 neurons, 0.0001 learning rate and 5000 epochs but at 3.36 seconds which is relatively higher.

As seen from the above discussed results, a balance is to be achieved while selecting settings for learning rate, number of hidden layers, number of neurons per layer, and number of epochs. Higher prediction accuracies need to be balanced with computational time for the predictive models. This is critical when applying the multilayer perceptron and related deep learning models for real-time implementations in manufacturing processes such as fused deposition based additive manufacturing. It was also revealed that higher number of hidden layers, or number of neurons and epochs may not always lead to "effective learning" and higher prediction accuracies. This can occur due to overfitting of model parameters to datasets. Thus, a judicious selection of hyperparameters is warranted and sensitivity analysis needs to be conducted for deep learning machine learning models based on the configuration of the process under consideration.

Table 2: RMSE and runtime values with 1 hidden layer and varying number of neurons, learning rate, and epoch

	Hidden Layer	Learning Rate		Dimension Accuracy Output			Porosity Output			Strength Output		
	H1	LR	Epoch	RMSE	Runtime	Status	RMSE	Runtime	Status	RMSE	Runtime	Status
0	3	0.001	5000	6.37	0.553	NL	10.13	0.531	NL	33	0.636	NL
1	3	0.0001	5000	1.96	1.327	L	3.19	1.301	L	5.37	1.479	L
2	3	0.00001	5000	1.9	2.070	L	3.24	2.076	L	5.39	2.258	L
3	3	0.001	15000	6.37	3.863	NL	10.13	3.941	NL	33	4.076	NL
4	3	0.0001	15000	1.97	5.661	L	3.19	5.848	L	5.37	5.897	L
5	3	0.00001	15000	1.92	7.462	L	3.21	7.741	L	5.38	7.714	L
6	3	0.001	25000	6.37	10.335	NL	10.13	10.825	NL	33	10.532	NL
7	3	0.0001	25000	1.97	13.223	L	3.19	13.826	L	5.37	13.488	L
8	3	0.00001	25000	1.92	16.170	L	3.19	16.703	L	5.37	16.289	L
9	5	0.001	5000	6.37	0.609	NL	10.13	0.608	NL	33	0.593	NL
10	5	0.0001	5000	1.96	1.410	L	3.19	1.426	L	5.37	1.368	L
11	5	0.00001	5000	1.9	2.239	L	3.24	2.219	L	5.39	2.146	L
12	5	0.001	15000	6.37	4.111	NL	10.13	4.162	NL	33	4.135	NL
13	5	0.0001	15000	1.97	5.985	L	3.19	6.089	L	5.37	5.986	L
14	5	0.00001	15000	1.92	7.893	L	3.21	8.015	L	5.37	7.895	L
15	5	0.001	25000	6.37	10.882	NL	10.13	11.009	NL	33	10.946	NL
16	5	0.0001	25000	1.97	13.992	L	2.15	14.163	L	5.37	13.932	L
17	5	0.00001	25000	1.92	17.027	L	3.19	17.158	L	5.37	16.990	L
18	8	0.001	5000	6.37	0.646	NL	10.13	0.610	NL	33	0.621	NL
19	8	0.0001	5000	1.97	1.478	L	3.19	1.500	L	5.37	1.436	L
20	8	0.00001	5000	1.9	2.387	L	3.25	2.333	L	5.39	2.258	L
21	8	0.001	15000	6.37	4.398	NL	10.13	4.309	NL	33	4.269	NL
22	8	0.0001	15000	1.97	6.392	L	3.19	6.329	L	5.37	6.247	L
23	8	0.00001	15000	1.92	8.435	L	3.21	8.312	L	5.38	8.265	L
24	8	0.001	25000	6.37	11.546	NL	10.13	11.508	NL	33	11.388	NL
25	8	0.0001	25000	1.97	14.680	L	3.19	14.714	L	5.37	14.549	L
26	8	0.00001	25000	1.92	17.841	L	3.2	17.904	L	5.37	17.671	L

Table 3: RMSE and runtime values with 2 hidden layers and varying number of neurons, learning rate, and epoch

	Hidden Layer		Learning Rate		Dimension Accuracy Output			Porosity Output			Strength Output		
	H1	H2	LR	Epoch	RMSE	Runtime	Status	RMSE	Runtime	Status	RMSE	Runtime	Status
0	3	3	0.001	5000	6.51	0.991	NL	10.99	0.979	NL	32.91	1.035	NL
1	3	3	0.0001	5000	1.89	2.192	L	3.59	2.165	L	7	2.213	NL
2	3	3	0.00001	5000	1.94	3.360	L	3.51	3.358	L	6.41	3.418	L
3	3	3	0.001	15000	2.08	6.417	NL	10.99	6.498	NL	32.91	6.459	NL
4	3	3	0.0001	15000	1.89	9.625	L	2.52	9.612	L	7	9.568	NL
...	...	...	...	...	...	...	...	...	...	...	...	...	...
76	8	8	0.0001	15000	6.51	11.277	NL	10.99	11.308	NL	32.91	11.011	NL

77	8	8	0.00001	15000	6.51	14.848	NL	10.99	15.029	NL	6.4	14.651	L
78	8	8	0.001	25000	6.51	20.511	NL	10.99	20.822	NL	32.91	20.453	NL
79	8	8	0.0001	25000	6.51	26.181	NL	10.99	26.536	NL	32.91	26.332	NL
80	8	8	0.00001	25000	6.51	31.902	NL	10.99	32.283	NL	6.4	32.039	L

Table 4: RMSE and runtime values with 3 hidden layers and varying number of neurons, learning rate, and epoch

	Hidden Layers			Learning Rate		Dimension Accuracy Output			Porosity Output			Strength Output		
	H1	H2	H3	LR	Epoch	RMSE	Runtime	Status	RMSE	Runtime	Status	RMSE	Runtime	Status
0	3	3	3	0.001	5000	6.17	1.539	NL	11.35	1.491	NL	32.41	1.496	NL
1	3	3	3	0.0001	5000	1.73	3.359	L	3.46	3.191	NL	32.41	3.151	NL
2	3	3	3	0.00001	5000	1.7	5.050	L	3.52	5.030	L	5.91	4.905	L
3	3	3	3	0.001	15000	6.17	9.701	NL	11.35	9.639	NL	32.41	9.560	NL
4	3	3	3	0.0001	15000	1.28	14.337	L	3.46	14.214	NL	32.41	14.138	NL
...	...	...	...	...	...	...	...	...	...	...	...	...	...	...
238	8	8	8	0.0001	15000	6.17	17.561	NL	11.35	17.687	NL	32.41	17.417	NL
239	8	8	8	0.00001	15000	6.17	23.289	NL	11.35	23.361	NL	32.41	23.064	NL
240	8	8	8	0.001	25000	6.17	32.234	NL	11.35	32.445	NL	32.41	32.059	NL
241	8	8	8	0.0001	25000	6.17	41.221	NL	11.35	41.401	NL	32.41	41.273	NL
242	8	8	8	0.00001	25000	6.17	50.195	NL	11.35	50.477	NL	32.41	50.337	NL

6. Conclusions

Hyperparameter tuning of additive manufacturing process was researched using fused deposition modeling as an illustrative case. Five critical FDM input process parameters were used to obtain three output parameter values via fractional factorial experiments. The dataset obtained were used to train the chosen multilayer perceptron deep learning algorithm. For each hyperparameter tuning, a predictive model was obtained. Also, both RMSE and runtime values were used to evaluate optimal set of hyperparameters for the chosen FDM output parameters (e.g., dimension accuracy, porosity, and strength). From our findings, no learning occurs at a learning rate of 0.001 irrespective of other chosen hyperparameters. Dimension accuracy improved from a RMSE of 1.90 to 1.73 with an increase in the number of hidden layers from 1 to 3 although the runtime increased marginally. Porosity improved from a RMSE value of 3.19 to 1.28 with an increase in the number of hidden layers from 1 to 3 but not with learning rate beyond 0.0001. Thus, a balance is to be attained between choice of hyperparameter settings between model prediction accuracy and computational time for it to be useful for real-time implementation. This research serves as a foundation for our future work in building an effective digital twin of FDM based additive manufacturing processes.

Acknowledgements

The authors would like to express their gratitude for funding support from the National Science Foundation (NSF CMMI Award #1663128, #2100739, #2100850), Defense Manufacturing Community Program and the Center of Excellence in Product Design and Advanced Manufacturing at North Carolina A&T State University.

References

[1] S. Parupelli, S. D.-A. journal of applied sciences, and undefined 2019, "A comprehensive review of additive manufacturing (3d printing): processes, applications and future potential," *par.nsf.gov*, Accessed: Apr. 04, 2022. [Online]. Available: https://par.nsf.gov/biblio/10124832.

[2] L. A. Verhoef, B. W. Budde, C. Chockalingam, B. García Nodar, and A. J. M. van Wijk, "The effect of additive manufacturing on global energy demand: An assessment using a bottom-up approach," *Energy Policy*, vol. 112, pp. 349–360, Jan. 2018, doi: 10.1016/j.enpol.2017.10.034.

[3] S. Wasti and S. Adhikari, "Use of Biomaterials for 3D Printing by Fused Deposition Modeling Technique: A Review," *Front. Chem.*, vol. 8, p. 315, May 2020, doi: 10.3389/fchem.2020.00315.

[4] Z. Yang, L. Jin, Y. Yan, and Y. Mei, "Filament breakage monitoring in fused deposition modeling using acoustic emission technique," *Sensors (Switzerland)*, vol. 18, no. 3, Mar. 2018, doi: 10.3390/s18030749.

[5] S. Desai, C. Dean, and Y. Desai, "Cyber-enabled concurrent material and process selection in a flexible design for manufacture paradigm," *Int. J. Adv. Manuf. Technol.*, vol. 97, no. 5–8, pp. 1719–1731, Jul. 2018, doi: 10.1007/S00170-018-2034-6.

[6] H. Elhoone, T. Zhang, M. Anwar, and S. Desai, "Cyber-based design for additive manufacturing using artificial neural networks for Industry 4.0," *Int. J. Prod. Res.*, vol. 58, no. 9, pp. 2841–2861, May 2020, doi: 10.1080/00207543.2019.1671627.

[7] M. Ogunsanya, J. Isichei, S. Parupelli, … S. D.-P., and undefined 2021, "In-situ droplet monitoring of inkjet 3D printing process using image analysis and machine learning models," *Elsevier*, Accessed: Apr. 04, 2022. [Online]. Available: https://www.sciencedirect.com/science/article/pii/S2351978921000524.

[8] T. Akter, S. D.-M. & Design, and undefined 2018, "Developing a predictive model for nanoimprint lithography using artificial neural networks," *Elsevier*, Accessed: Apr. 04, 2022. [Online]. Available: https://www.sciencedirect.com/science/article/pii/S0264127518307597.

[9] H. Almakaeel, A. Albalawi, S. D.-M. Letters, and undefined 2018, "Artificial neural network based framework for cyber nano manufacturing," *Elsevier*, Accessed: Apr. 04, 2022. [Online]. Available: https://www.sciencedirect.com/science/article/pii/S2213846317300949.

[10] F. W. Baumann, A. Sekulla, M. Hassler, B. Himpel, and M. Pfeil, "Trends of machine learning in additive manufacturing," *Int. J. Rapid Manuf.*, vol. 7, no. 4, p. 310, 2018, doi: 10.1504/ijrapidm.2018.095788.

[11] J. Zhang, P. Wang, and R. X. Gao, "Deep learning-based tensile strength prediction in fused deposition modeling," *Comput. Ind.*, vol. 107, pp. 11–21, 2019, doi: 10.1016/j.compind.2019.01.011.

[12] D. Wu, Y. Wei, and J. Terpenny, "Surface roughness prediction in additive manufacturing using machine learning," *ASME 2018 13th Int. Manuf. Sci. Eng. Conf. MSEC 2018*, vol. 3, 2018, doi: 10.1115/MSEC2018-6501.

[13] Z. Li, Z. Zhang, J. Shi, and D. Wu, "Prediction of surface roughness in extrusion-based additive manufacturing with machine learning," *Robot. Comput. Integr. Manuf.*, vol. 57, pp. 488–495, 2019, doi: 10.1016/j.rcim.2019.01.004.

[14] S. H. Rahul, K. Balasubramanian, and S. Venkatesh, "Optimizing inkjet printing process to fabricate thick ceramic coatings," *Ceram. Int.*, 2017, doi: 10.1016/j.ceramint.2016.12.103.

[15] L. Cao, J. Li, J. Hu, H. Liu, Y. Wu, and Q. Zhou, "Optimization of surface roughness and dimensional accuracy in LPBF additive manufacturing," *Opt. Laser Technol.*, vol. 142, p. 107246, Oct. 2021, doi: 10.1016/j.optlastec.2021.107246.

[16] C. Xia, Z. Pan, J. Polden, H. Li, Y. Xu, and S. Chen, "Modelling and prediction of surface roughness in wire arc additive manufacturing using machine learning," *J. Intell. Manuf.*, 2021, doi: 10.1007/s10845-020-01725-4.

[17] G. Tapia, A. H. Elwany, and H. Sang, "Prediction of porosity in metal-based additive manufacturing using spatial Gaussian process models," *Addit. Manuf.*, vol. 12, pp. 282–290, 2016, doi: 10.1016/j.addma.2016.05.009.

[18] S. Ho *et al.*, "DLAM: Deep Learning Based Real-Time Porosity Prediction for Additive Manufacturing Using Thermal Images of the Melt Pool," *IEEE Access*, vol. 9, pp. 115100–115114, 2021, doi: 10.1109/ACCESS.2021.3105362.

[19] J. Bartolai, T. W. Simpson, and R. Xie, "Predicting strength of thermoplastic polymer parts produced using additive manufacturing," *Solid Free. Fabr. 2016 Proc. 27th Annu. Int. Solid Free. Fabr. Symp. - An Addit. Manuf. Conf. SFF 2016*, pp. 951–963, 2016, Accessed: Jan. 10, 2022. [Online]. Available: http://utw10945.utweb.utexas.edu/sites/default/files/2016/077-Bartolai.pdf.

[20] J. Bergstra and Y. Bengio, "Random search for hyper-parameter optimization," *J. Mach. Learn. Res.*, vol. 13, pp. 281–305, 2012, Accessed: Jan. 18, 2022. [Online]. Available: https://www.jmlr.org/papers/volume13/bergstra12a/bergstra12a.

[21] B. Shahriari, K. Swersky, Z. Wang, R. P. Adams, and N. De Freitas, "Taking the human out of the loop: A review of Bayesian optimization," *Proc. IEEE*, vol. 104, no. 1, pp. 148–175, 2016, doi: 10.1109/JPROC.2015.2494218.